PAPER

Check for updates

A pH-responsive dual-network biopolysaccharide hydrogel with enhanced self-healing and controlled drug release properties

Yuan Ma,[a] Yunfeng Tang,[b] Jianwei Fan,[b] Tianyu Sun,[c] Xiaoyong Qiu, [ID] [a] Luxing Wei[d] and Xiaolai Zhang [ID] *[a]

Traditional hydrogels based on Schiff base reactions frequently encounter issues with rapid drug release when employed as drug delivery systems owing to their susceptibility to hydrolysis under acidic conditions. It is, therefore, necessary to implement improvements to regulate the drug release behavior. In this study, a dual-network and pH-responsive biopolysaccharide hydrogel was developed, which is self-healing, injectable and biocompatible. Most importantly, the hydrogel has excellent tunability for controlled drug release. The hydrogel consisted of a primary network of dibenzaldehyde-functionalized poly(ethylene glycol) (DP) and chitosan (CS) formed through a Schiff base reaction and a secondary network of sodium alginate (SA) and CS formed through electrostatic interactions. It was found that the DP–CS–2%SA hydrogel can prolong the release duration up to four-fold compared to the single-network DP–CS hydrogel at a given release threshold. Significantly, by adjusting the relationship between the two effects through the amount of SA, the release modifiability of drug delivery systems has been greatly enhanced. This study could significantly enhance the tunability of hydrogel drug delivery systems.

1. Introduction

The rapid development of biomaterial science and pharmaceutical engineering has led to the emergence of drug delivery systems as a significant branch of modern healthcare. Among the numerous materials employed in the field of drug delivery, hydrogels have attracted considerable attention owing to their biodegradability, biocompatibility, and non-toxicity.[1] The pH value of the human body tends to vary in different tissues and organs. For example, the stomach presents an acidic environment, while the pH of the intestine is close to neutral.[2] Some responsive hydrogels can respond to changes in pH, temperature, and ions,[3,4] and precisely, this property can be exploited to design an acid-sensitive hydrogel so that the drug it carries will be released most in the therapeutic site, thus exerting therapeutic effects.

However, the traditional single-network hydrogel has limitations in terms of mechanical strength and drug-release control, which to some extent restrict their long-term stable application in drug delivery systems. For example, a pH-

responsive hydrogel is formed by the Schiff base cross-linking of chitosan (CS) with aldehyde compounds.[5] Under acidic conditions, Schiff base-based hydrogels undergo a chemical reaction in which the protonated nitrogen atoms in the Schiff base react with acid protons to form amino cations and carbonium ions. This process results in the protonation of amino groups, leading to the formation of a stable intermediate. In this state, the carbonium ion is susceptible to nucleophilic attack by water, which cleaves the Schiff base bonds,[5,6] causing the gel network to break down and release the encapsulated drug. Because of this issue, Schiff base cross-linked hydrogels have some drawbacks in drug release, such as being prone to breakage under acidic conditions, which may lead to premature release or instability of the drug.[7] In Zhou's research, a thermosensitive hydrogel loaded with Ba–HP–CD complexes achieved a 100% release rate within 7 hours, with complete release before reaching the lesion site.[8]

In recent years, there has been significant progress in research on the structural strengthening and controlled drug release of hydrogels by constructing a dual-network. For example, in Huang's study, a graphene oxide-filled CS-based network serves as the first network and a polyacrylamide network serves as the second network, enhancing the mechanical properties of the hydrogel.[9] Chen studied a chitosan/dialdehyde sodium alginate/magnetic dopamine hydrogel with excellent targeted drug delivery and controlled-release properties.[10] Furthermore, we revealed that electrostatic interactions and intermolecular hydrogen bonding lead to pH

[a]*School of Chemistry and Chemical Engineering, Shandong University, Jinan 250100, China. E-mail: zhangxlai@sdu.edu.cn*

[b]*Lunan Pharmaceutical Group Co., Ltd., Linyi 273400, China*

[c]*Jinan Children's Hospital, Jinan 250022, China*

[d]*Key Laboratory of High Efficiency and Clean Mechanical Manufacture of Ministry of Education, School of Mechanical Engineering and Advanced Medical Research Institute, Shandong University, Jinan, Shandong 250061, China*

sensitivity opposite to that of Schiff base bonds. Under acidic conditions, the amine groups of chitosan become further protonated, which enhances the electrostatic interactions and intermolecular hydrogen bonding between chitosan and sodium alginate (SA). This increased interaction slows down the release of the drug.[11,12] Therefore, we introduced SA on the basis of a chitosan network to enhance the controlled-release properties of the hydrogel.

CS is a biopolymer derived from the deacetylation of chitin and possesses two reactive functional groups: an amine group and an additional hydroxyl group. These functional groups enable the formation of cross-links between polymer chains, as described in ref. 13. Furthermore, CS exhibits many inherent properties, including biocompatibility and biodegradability.[14] SA is a biocompatible and biodegradable anionic linear polysaccharide extracted from algae. SA hydrogel has a structure similar to the extracellular matrix of mammalian tissues, which is essentially composed of a hydrated network of proteins and polysaccharides to support cells. Therefore, in tissue engineering applications, SA hydrogel is employed as a carrier to deliver bioactive substances such as small chemical drugs, proteins, and cells.[15] The negatively charged carboxyl groups on SA chains can combine with the positively charged amine groups of protonated CS under the influence of electrostatic forces to form a network structure.[16] The double-network hydrogel provides adjustable pH-responsive properties, with the drug release rate controlled by regulating the amount of SA used. Baicalin (BC) is a traditional Chinese medicine known for its antimicrobial and anti-inflammatory properties.[17] To investigate the practical application of drug-loaded hydrogels, we have selected BC as the subject to examine the drug-controlled release performance and application of hydrogels.

In this study, we prepared a self-healing CS–SA-based double-network hydrogel by incorporating SA into the DP–CS hydrogel through Schiff base reaction and electrostatic interaction. This treatment not only enhanced the mechanical strength of hydrogels but also enabled controlled drug release. We investigated the effect of SA content on the structure and properties of the hydrogel. Scanning electron microscopy (SEM) and Fourier transform infrared spectroscopy (FTIR) were used to characterize the structure of the DP–CS–2%SA hydrogel. The storage (G') and loss (G'') moduli of the DP–CS–2%SA hydrogel were measured. In vitro drug-release performance, biocompatibility, and antimicrobial activity were evaluated using BC as a model drug. Compared with the single-network DP–CS hydrogel, the DP–CS–2%SA hydrogel exhibits superior structural strength, injectability, self-healing properties, and the ability to achieve more precise drug control release. This study conducted a comprehensive investigation and evaluation of the applications of the DP–CS–2%SA hydrogel as a drug carrier for controlled drug release.

2. Materials and methods

2.1. Materials

CS (M_w = 150 000), SA, anhydrous $CaCl_2$ (96%), phosphate-buffered saline (PBS) buffer solution (pH = 3, 5, and 7), and dimethyl sulfoxide (DMSO, analytical grade) were purchased from Shanghai Macklin Biochemical Co., Ltd (Shanghai, China). Polyethylene glycol (PEG, M_w = 2000) and tetrahydrofuran (THF, analytical grade) were obtained from the China National Medicines Group Chemical Reagents Co., Ltd (Shanghai, China). N,N'-Dicyclohexylcarbodiimide (DCC, purity 99%), 4-(dimethylamino) pyridine (DMAP, purity 99%) and 4-formylbenzoic acid (purity 98%) were purchased from Shanghai Aladdin Biochemical Technology Co., Ltd (Shanghai, China). Baicalin (purity 98%) was procured from Chengdu Derick Biotechnology Co., Ltd (Chengdu, China). Distilled water was used for solution preparation.

2.2. Preparation of dibenzaldehyde polyethylene glycol (DFPEG)

The following procedure was performed in a fume hood: PEG (8 g), 4-formylbenzoic acid (1.8 g), and DMAP (0.18 g) were dissolved in a round-bottom flask containing 100 mL of THF. The solution was subjected to ultrasonic treatment until the solutes were completely dissolved (Solution A). Next, 3.296 g of DCC was dissolved in a round-bottom flask containing 60 mL of THF (Solution B).

Nitrogen gas was introduced for approximately 10 minutes to purge any residual gases from Solutions A and B. Solution B was then slowly injected into Solution A using a syringe. The resulting mixture was stirred with a magnetic stirrer for 24 hours. After 24 hours, the mixture was filtered to remove any solid particles. The filtrate was evaporated under reduced pressure to remove the organic solvent from the product. The remaining product was dissolved in distilled water and filtered to remove insoluble impurities. Ultimately, the filtrate was subjected to lyophilization to yield a white powder form of DFPEG.

2.3. Preparation of the CS single-network hydrogel

Firstly, 0.5 g of CS was added to 24.5 mL of 2% glacial acetic acid solution, and the mixture was ultrasonically stirred until the CS was completely dissolved, resulting in a 2% CS solution. BC was dissolved in DMSO to obtain a 20 mg per mL BC solution. DFPEG was dissolved in pure water to obtain a 10% DFPEG solution.

The DFPEG solution was mixed with the BC solution. This mixture was labeled as Solution 1. Solution 1 was combined with the 2% CS solution, stirred thoroughly, and poured into a mold to solidify the resulting DP–CS hydrogel.

2.4. Preparation of the CS–SA double-network pH-responsive hydrogel

As described above, a 2% CS solution and 20 mg per mL baicalin solution were prepared.

SA was dissolved in 10% DFPEG solution to obtain a DFPEG aqueous solution with different concentrations of SA. The DFPEG and SA mixed solution was mixed evenly with baicalin solution and labeled as Solution 2. Solution 2 was combined with 2% CS solution with 10% $CaCl_2$ and stirred thoroughly. The mixture was poured into a mold to be solidified, resulting
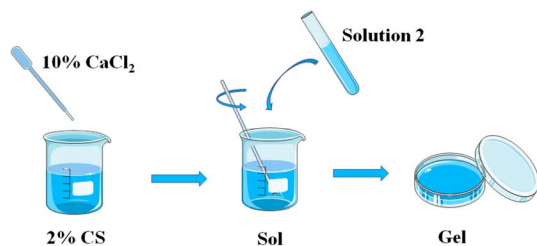
Fig. 1 Preparation process of the DP–CS–SA hydrogel.

Table 1 Parameters for the preparation of different hydrogels

Hydrogel	CS (wt%)	DFPEG (wt%)	SA (wt%)	CaCl$_2$ (wt%)
DP–CS	2	10	0	2
DP–CS–1%SA	2	10	1	2
DP–CS–2%SA	2	10	2	2

in hydrogels (DP–CS–1%SA and DP–CS–2%SA) with different concentrations of DP–CS–SA. Fig. 1 shows the preparation process of the DP–CS–SA hydrogel (Table 1).

2.5. Characterization methods

FTIR (Thermo Scientific Nicolet iS20, USA), SEM (Hitachi Regulus8100, Sigma 300), rheometer (MCR302, Anton Paar, Austria), and UV-Vis-NIR spectrophotometry (CARY5000) were used to analyze the chemical structure, morphological structure, storage modulus (G'), loss modulus (G''), and *in vitro* drug release of the synthesized hydrogel samples.

2.6. Rheological tests

A rheometer was employed to perform variable strain and frequency sweeps on the DP–CS, DP–CS–1%SA, and DP–CS–2% SA hydrogels with a 25 mm cone-plate geometry, recording the changes in the G' and G'' of the hydrogel. At 1% strain, a frequency sweep was performed over the hydrogel in the frequency range of 1–100 Hz. The strain amplitude sweep of the hydrogel coating samples was executed in the strain range of 0.01–100% at a frequency of 1 Hz. Simultaneously, continuous step strain measurements were performed on the hydrogel materials at a frequency of 1 Hz, with the strain moving between $\gamma = 1\%$ and $\gamma = 600\%$ at 100 s intervals.

2.7. Swelling tests

To investigate the swelling properties of the DP–CS–SA hydrogel, it was freeze-dried for 24 hours and then immersed in PBS at 25 °C. The hydrogel was removed every 30 minutes, and its surface moisture was blotted with filter paper. The weight was measured and recorded. The swelling ratio ε is calculated using eqn (1):

$$\varepsilon = \frac{(W_t - W_0)}{W_0} \times 100\% \tag{1}$$

W_t is the weight of the hydrogel at time t (g), and W_0 is the initial weight of the hydrogel (g).

2.8. *In Vitro* release tests

To evaluate the *in vitro* release profiles of the baicalin-loaded DP–CS–SA hydrogel, the baicalin-loaded hydrogel was immersed in 10 mL of PBS solutions at different pH values (pH = 3, 5, and 7). The absorbance of baicalin in PBS was recorded over time using a UV-Vis-NIR spectrophotometer. The intensity of the absorption peak of baicalin at 278 nm was monitored.

Standard solutions of baicalin were prepared at different concentrations. These solutions were scanned using a UV-Vis-NIR spectrophotometer in the wavelength range of 200–400 nm. The absorbance was recorded at 278 nm to construct a standard curve of the UV absorption of baicalin.

2.9. Biocompatibility tests

As described in the previous studies,[18] the biocompatibility of the hydrogel was assessed using the Cell Counting Kit-8 (CCK-8) method. Hydrogel pieces (0.4 g) were placed in 2 mL of the culture medium and allowed to soak for 48 h to obtain the liquid extract. L929 cells were cultured in a 96-well plate, and the liquid extract was added to the 96-well plate. After co-culturing for 1 or 3 days, 100 μL of the culture medium containing 10% CCK-8 solution was added, and the biocompatibility of the cells was assessed using the CCK-8 method. The absorbance was monitored at 450 nm using a microplate reader.

The following formula was used to calculate cell viability (%):

$$\text{Vitality } (\%) = \frac{A}{B} \times 100\% \tag{2}$$

A represents the absorbance of the test sample, and B represents the absorbance of the control sample.

2.10. Antibacterial activity tests

As previously described in this study, *Staphylococcus aureus* was selected as a representative bacterium to assess the antibacterial activity of the baicalin-loaded hydrogel using inhibiting ring tests.[19] The hydrogel was placed on a culture dish, which was then covered with bacteria and incubated at 37 °C for 24 hours. The diameter of the inhibition zone was then measured.

3. Results and discussion

3.1. Hydrogel preparation

The double-network structure of the DP–CS–SA hydrogel was formed by a combination of Schiff base reactions and electrostatic interactions, as illustrated in Fig. 2. The CS amine groups reacted with the aldehyde groups at both ends of DFPEG to form a three-dimensional network structure through covalent bonds. Fig. 2 illustrates the drug-release process from the hydrogel.[20,21] Simultaneously, the protonated amine groups were attracted to the carboxyl groups,[3] forming the second network structure of the DP–CS–SA hydrogel under the influence of electrostatic forces. The remaining SA, which did not react, cross-linked with calcium ions *via* ionic exchange and stabilizing the structure of the hydrogel.[22]
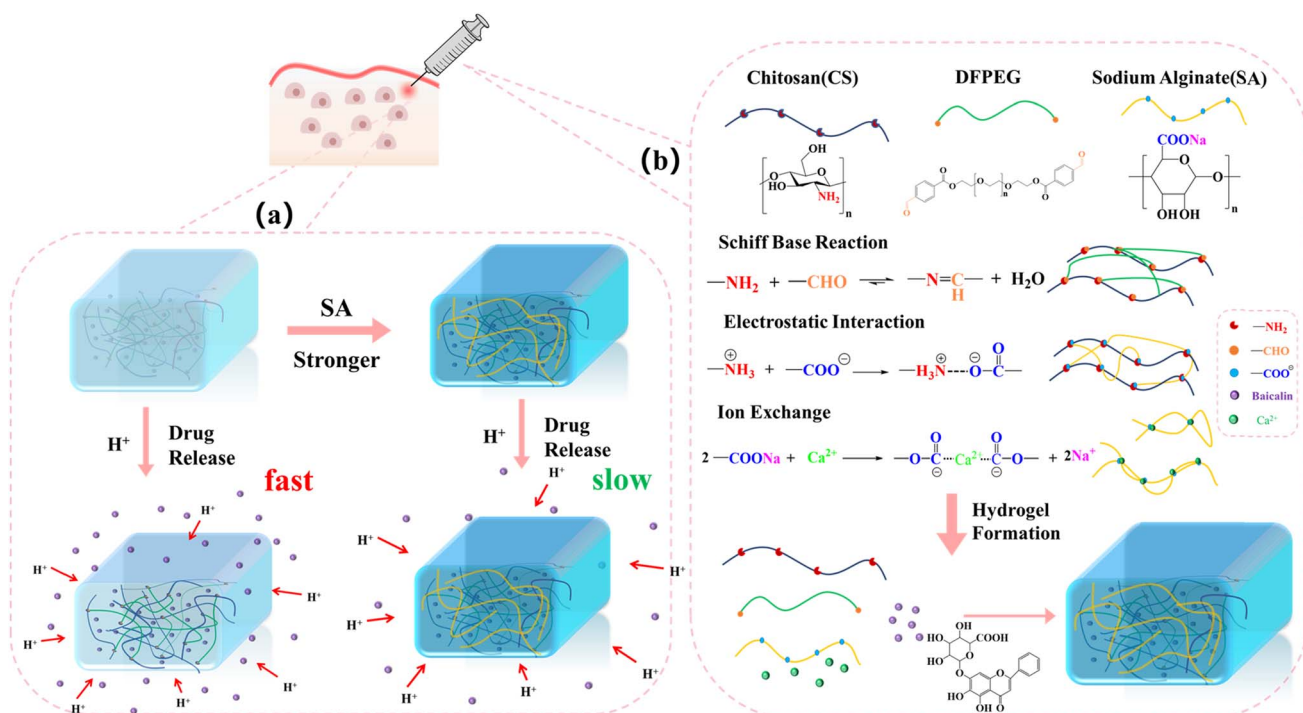
Fig. 2 (a) Schematic of the drug release process of DP–CS–SA and DP–CS; (b) schematic of the preparation process of DP–CS–SA.

The DP–CS–SA hydrogel was pH sensitive. Under acidic conditions, hydrogen ions undergo protonation with nitrogen atoms in the Schiff base bonds, forming positively charged nitrogen ions. Subsequently, water molecules attacked these positively charged nitrogen ions, breaking the carbon-nitrogen bonds to form acids and amines. As the Schiff base bonds broke, the hydrogel disintegrated, allowing drug molecules to release and diffuse from the inside to the outside of the hydrogel.[6,23] The combination of SA and CS through electrostatic interactions forms a structure insensitive to pH fluctuations.[23,24] Even under acidic conditions, the hydrogel maintained a certain three-dimensional network structure, achieving controlled drug release under acidic conditions.

3.2. FTIR and SEM analysis

Fig. 3(a) shows images demonstrating the DP–CS–2%SA hydrogel before and after cross-linking, confirming its ability to cure in a short period. Fig. 3(b–d) shows SEM images of the DP–CS, DP–CS–1%SA, and DP–CS–2%SA hydrogel. All three hydrogels have a porous and reticular structure. However, with the introduction of SA, the number of pores and the pore size decreased. Therefore, it could be inferred that the incorporation of SA affects the porous structure of the hydrogel, making it more compact and uniform. As shown in Fig. 3(e–g), the baicalin-loaded hydrogels exhibited smaller internal pore structures, indicating that baicalin was successfully dispersed in the hydrogel.

Fig. 3(h) shows the FTIR spectral analysis results for the SA, CS, and DP–CS–2%SA hydrogel. The characteristic absorption peak of CS, as indicated by the yellow curve, is at 890 cm^{-1}, caused by the stretching vibration of the pyranose ring. The absorption peaks at 1590 and 1644 cm^{-1} correspond to the N–H of protonated amino and primary amine groups, respectively.[25] In the FTIR spectrum of SA (Fig. 3(h), green curve), the characteristic absorption peaks at 1616 and 1418 cm^{-1} correspond to the asymmetric and symmetric stretching vibrations of the –COO group, respectively.[26] After cross-linking CS with DFPEG, a Schiff base absorption peak appeared at 1644 cm^{-1} (Fig. 3(h), blue curve), corresponding to the characteristic vibration of the imine C=N bond.[27] The FTIR spectrum shows that the CS amide and SA carboxylate anion form a broad band between 1566 and 1660 cm^{-1}, confirming the characteristic peak of the electrostatic interaction between SA and CS (Fig. 3(h), red curve). The disappearance of the N–H bending vibration of the CS primary amine (1590 cm^{-1}) and the asymmetric and symmetric –COO stretching vibrations of SA (1418 cm^{-1}) indicate that the ($-NH_3^+$) of CS reacted with the ($-COO$) of SA.[28] Fig. 3(i) shows the infrared spectra of the DP–CS–2%SA–BC hydrogel, DP–CS–2%SA hydrogel, and baicalin. The yellow curve represents the infrared absorption curve of baicalin, which shows characteristic peaks for the –OH stretching at 3552 and 3493 cm^{-1}, for the carbonyl group (>C=O) at 1726 and 1660 cm^{-1}, and for the C–O–C in the ether and hydroxyl groups at 1076 cm^{-1}.[29] The green curve shows the infrared spectrum of the baicalin-loaded DP–CS–2%SA hydrogel; however, due to the low content of baicalin in the hydrogel, the characteristic absorption peaks of baicalin were not distinct.[30]

3.3. Swelling analysis

Tissues and other body fluids are the primary environments in which hydrogels function in biomedical applications.[10]
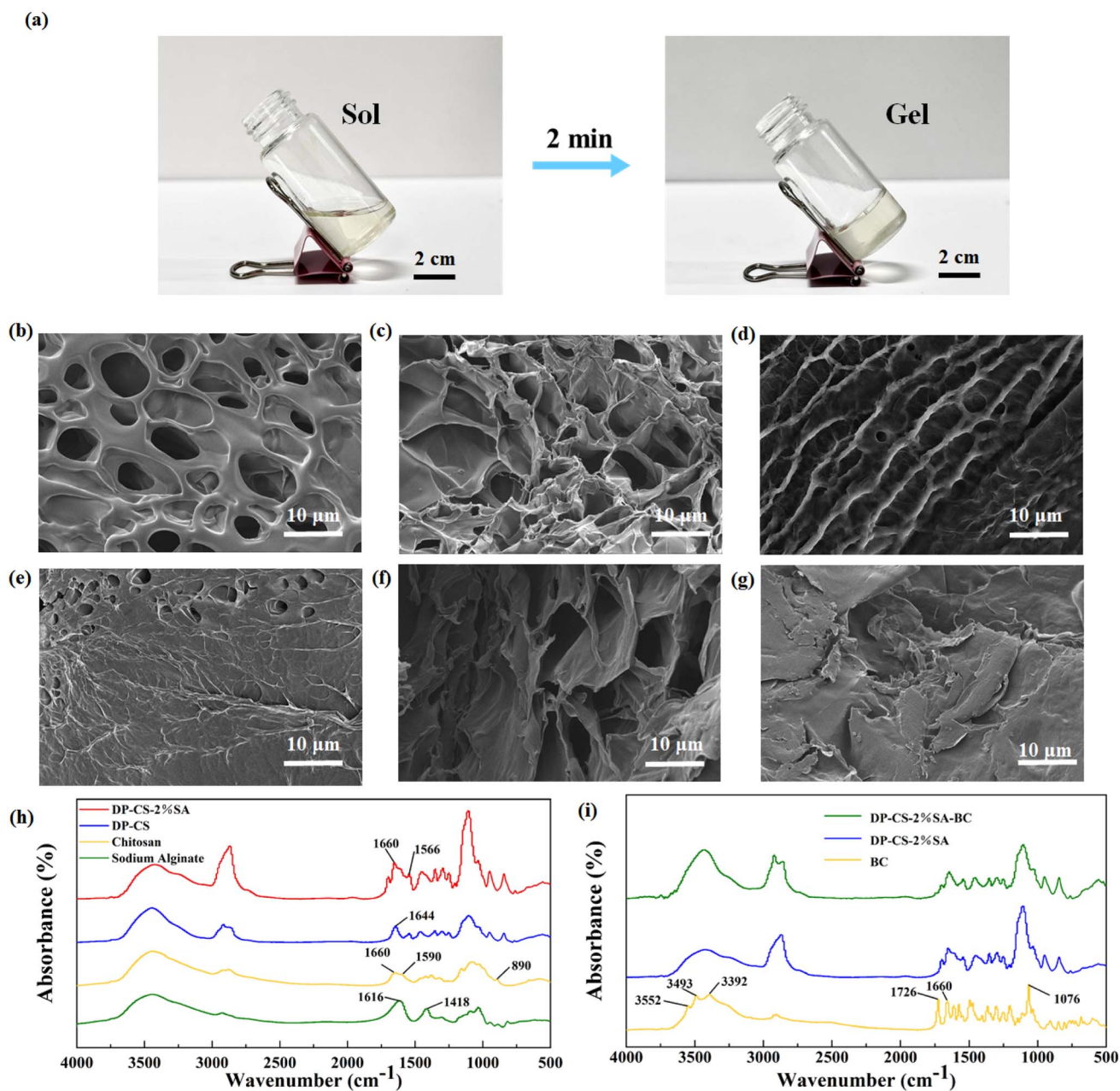
Fig. 3 (a) Photographs of the gelation process of the DP−CS−2%SA hydrogel; (b)−(d) scanning electron microscopy (SEM) images of blank DP−CS, DP−CS−1%SA, and DP−CS−2%SA hydrogel samples; (e)−(g) SEM images of baicalin-loaded DP−CS, DP−CS−1%SA, and DP−CS−2%SA hydrogel samples; (h) FTIR spectra of sodium alginate, chitosan, DP−CS, and DP−CS−2%SA hydrogel; (i) FTIR spectra of BC, DP−CS−2%SA−BC and DP−CS−2%SA.

Consequently, studying the mass differences between dry and wet states is very meaningful. The freeze-dried DP−CS, DP−CS−1%SA, and DP−CS−2%SA hydrogels were soaked in PBS (pH = 7) to study their swelling properties. As shown in Fig. 4(a), the DP−CS hydrogel exhibited the fastest swelling rate, with the swelling ratio approaching 100% after approximately 1 hour and reaching approximately 200% after approximately 4 hours, after which it tended to stabilize. In contrast, the DP−CS−1%SA and DP−CS−2%SA hydrogel exhibited a swelling rate of only 60% within the first hour, reaching 90% and 80%, respectively, after

approximately 3 hours and tended to stabilize. The DP−CS hydrogel exhibited the highest swelling capacity. In general, the swelling capacity of a hydrogel depends on its porous structure and the degree of cross-linking. This is because a double-network structure formed by SA and CS increases the degree of cross-linking of the hydrogel, which increases its mechanical stability but reduces its swelling capacity.[10,31] In summary, the swelling performance of DP−CS−1%SA and DP−CS−2%SA in simulated body fluids was lower than that of DP−CS. However, both formulations still had sufficient water absorption capacity
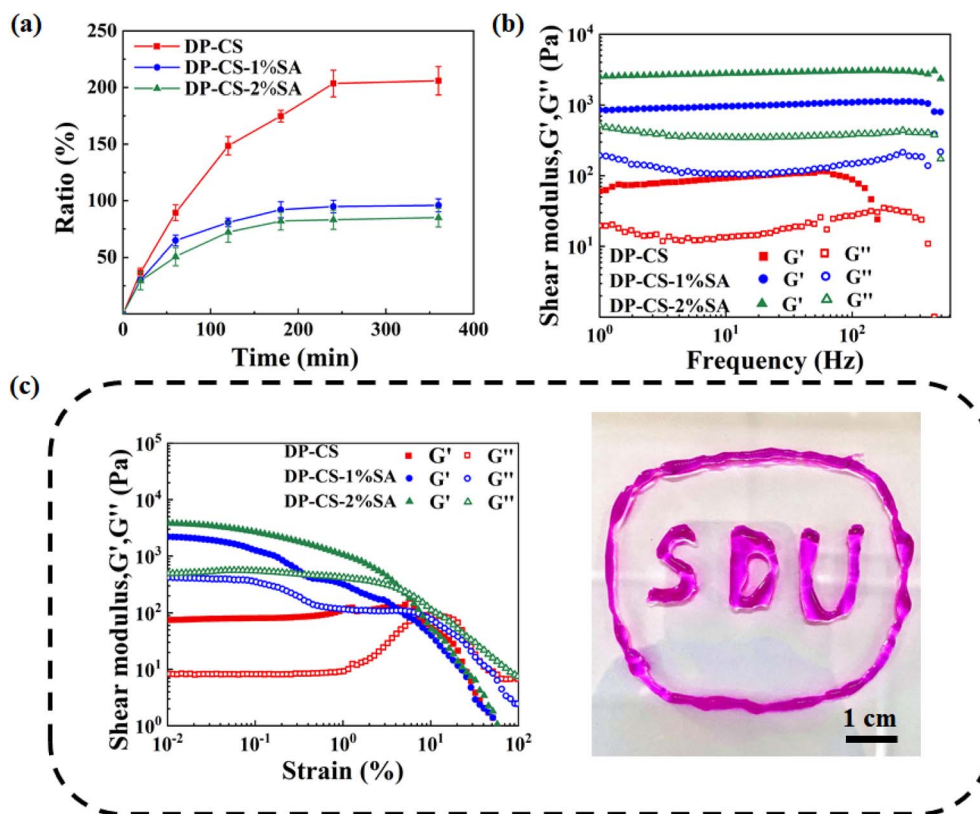
Fig. 4   (a) Swelling ratios of the DP–CS, DP–CS–1%SA, and DP–CS–2%SA hydrogel samples over time in PBS (pH = 7.4) at 37 °C; (b) frequency sweep tests of DP–CS, DP–CS–1%SA, and DP–CS–2%SA hydrogel samples; (c) strain sweep tests of DP–CS, DP–CS–1%SA, and DP–CS–2%SA hydrogel samples and the pattern extruded from the DP–CS–2%SA.

to achieve controlled drug release. This property ensured stability during long-term use and storage, preventing deformation or failure. The drug-release rate could be better controlled, which is beneficial for achieving sustained and stable therapeutic effects.

3.4.   Rheological analysis

To investigate the rheological properties of the hydrogel, the G' and G'' values of DP-CS, DP-CS-1%SA, and DP-CS-2%SA were measured under different conditions. As shown by the red curve in Fig. 4(b), at lower shear frequencies (below 100 Hz), G' was greater than G'', indicating that DP–CS is an elastic hydrogel. At higher shear frequencies (above 100 Hz), G' was less than G'', and the hydrogel exhibited pseudoplastic behavior.[14] The green and blue curves in Fig. 4(b) show that the DP–CS–1%SA and DP–CS–2%SA hydrogels maintain their solid states at shear frequencies above 100 Hz. This indicates that the G' and G'' values of DP–CS–1%SA and DP–CS–2%SA significantly increased compared with those of DP–CS. This phenomenon suggests that the DP–CS–1%SA and DP–CS–2%SA hydrogels have higher cross-linking densities than the DP–CS hydrogel. Consistent with the SEM results shown in Fig. 2, this result was due to the double-network interaction between SA and CS.

As shown in Fig. 4(c), the G' and G'' of DP-CS-1%SA and DP-CS-2%SA hydrogels remained unchanged at low strains, but when the strain exceeded 0.2%, both the G' and G'' decreased

rapidly. They cross at a strain of 5%, indicating that the gel network was damaged. For the DP–CS hydrogel, G' and G'' remained constant at strains <1%, but when the strain exceeded 10%, they decreased rapidly and G' became lower than G'', indicating that the hydrogel structure began to be destroyed when the strain exceeded 10%. In addition, the G' and G'' values of both DP-CS-1%SA and DP-CS-2%SA were higher than those of DP–CS, indicating that the mechanical strength of DP–CS–1%SA and DP–CS–2%SA is higher than that of DP–CS. At the same time, for all three hydrogels, G' decreased rapidly at higher strains, with G'' finally exceeding G', indicating that they exhibit shear thinning properties at high strains, implying that their viscosity decreases with increasing strain.[31,32] This property imparted injectability to the hydrogel. Fig. 4(c) shows the pattern extruded from a syringe filled with DP–CS–SA, demonstrating its injectability, which helps the material to serve as an important material in the medical field and be applicable in various medical settings.

3.5.   Self-healing analysis

The self-healing performance of hydrogels refers to their ability to self-repair and restore their original structure after damage, effectively extending their life. Rheological experiments were performed to determine the changes in G' and G'' in DP-CS, DP-CS-1%SA, and DP-CS-2%SA under alternating strains of 1% and 600%. As shown in Fig. 5(a), when the strain was switched
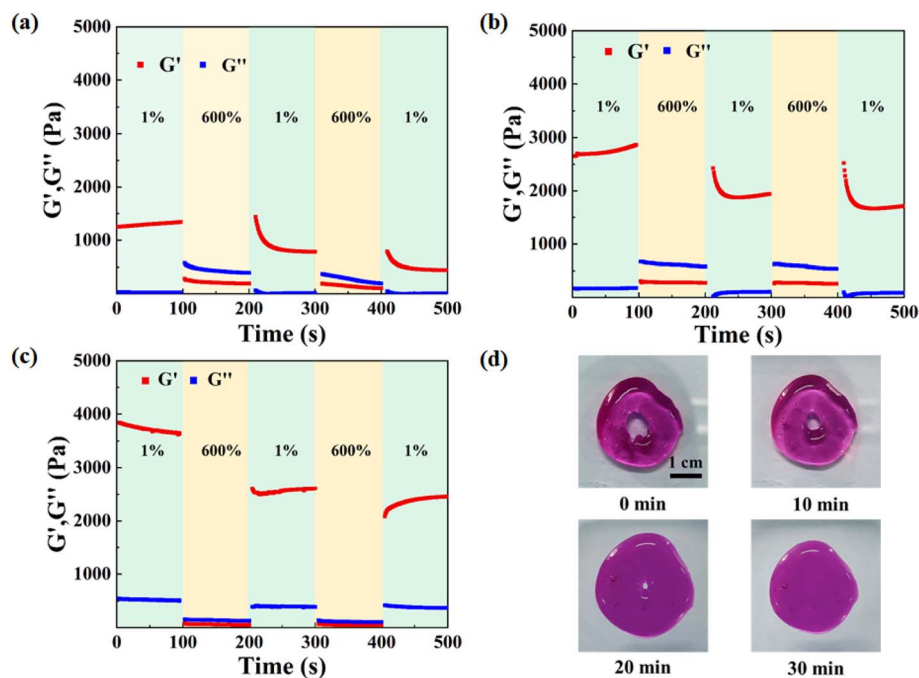
Fig. 5 (a)–(c) Changes in the shear modulus of DP–CS, DP–CS–1%SA, and DP–CS–2%SA hydrogel samples during strain step cycling from 1% to 600%; (d) morphological changes in the DP–CS–2%SA hydrogel at different time intervals.

from 1% to 600%, the G' value of the DP–CS sample decreased sharply, and the G'' value increased abruptly and exceeded the G' value, indicating that the internal structure of DP–CS was damaged. When the strain suddenly switched back to 1% from 600%, the G' value of the DP–CS was slightly lower than before, indicating that the internal network structure of DP–CS was essentially restored.[33–35] After three cycles of strain mutation, a gradual decrease in G' in DP–CS indicated a decline in its self-healing performance. Fig. 5(b and c) show that DP–CS–1%SA and DP–CS–2%SA exhibited a decrease in G' value after one cycle of the strain mutation. However, in subsequent cycles, the G' value gradually stabilized. This result may be caused by the good adhesive properties of SA and its inherent gel nature.[36,37] When the hydrogel is fractured or damaged, SA adheres to the fracture surface and forms a temporary hydrogel layer *via* gelation, playing a supporting and connecting role. This indicates that adding SA enhances the self-healing ability of DP–CS–1%SA and DP–CS–2%SA.

Fig. 5(d) shows photographs of the self-healing performance test of the DP–CS–2%SA hydrogel stained with rhodamine B. Initially, a 0.5 cm circular hole was observed in the middle of the DP–CS hydrogel block. After 10 minutes, the hole shrinks to 0.2 cm, and after 30 minutes, the hole is completely healed. These results further demonstrate that the DP–CS–2%SA hydrogel has excellent self-healing properties.

3.6. *In Vitro* drug-release analysis

Baicalin is a natural drug with antimicrobial properties, but there is a relative lack of research on its hydrogel-loaded drug release. To verify the feasibility of DP–CS, DP–CS–1%SA, and DP–CS–2%SA hydrogels for the controlled release of baicalin, *in*

vitro drug-release experiments were conducted. The release rate of baicalin was determined using a standard calibration curve. Fig. 6(a–c) shows the release rates of baicalin from DP–CS, DP–CS–1%SA, and DP–CS–2%SA at different pH values.

The effect of pH on drug release from the hydrogel was investigated, and the release profiles of DP–CS, DP–CS–1%SA, and DP–CS–2%SA hydrogels at different pH levels over time are shown in Fig. 6(a–c). Within the first 3 h, the release rate of baicalin was relatively faster at lower pH levels. The release rates of DP–CS, DP–CS–1%SA, and DP–CS–2%SA hydrogels at pH = 3 could reach 90%, 60%, and 40%, respectively, after 4 h. Under pH = 5, the release rates of the three samples after 4 h were 28%, 20%, and 13%, respectively. At pH = 7, the release rates of the three samples after 4 h were only approximately 5%. After 12 h, the release rates of all three samples reached their maximum values. With decreasing pH, the release rate and speed of baicalin from DP–CS, DP–CS–1%SA, and DP–CS–2%SA hydrogels gradually increased due to the cleavage of Schiff base bonds. Therefore, the release rate of baicalin can be controlled by changing the pH of the environment.

The augmentation of hydrogen ions facilitates the protonation of amino groups within chitosan under acidic conditions. This increased protonation intensifies the electrostatic interactions between CS and SA. As a result, the degradation of the gel matrix is effectively mitigated. Fig. 6(d–f) shows the release rate trends of DP–CS, DP–CS–1%SA, and DP–CS–2%SA at pH 3, 5, and 7, respectively. It can be observed from Fig. 5 that under acidic conditions, the release rates of DP–CS, DP–CS–1%SA, and DP–CS–2%SA become increasingly clear. After 4 hours, the release rates of baicalin for DP–CS, DP–CS–1%SA, and DP–CS–2%SA were 91%, 57%, and 41%, respectively. However, with the
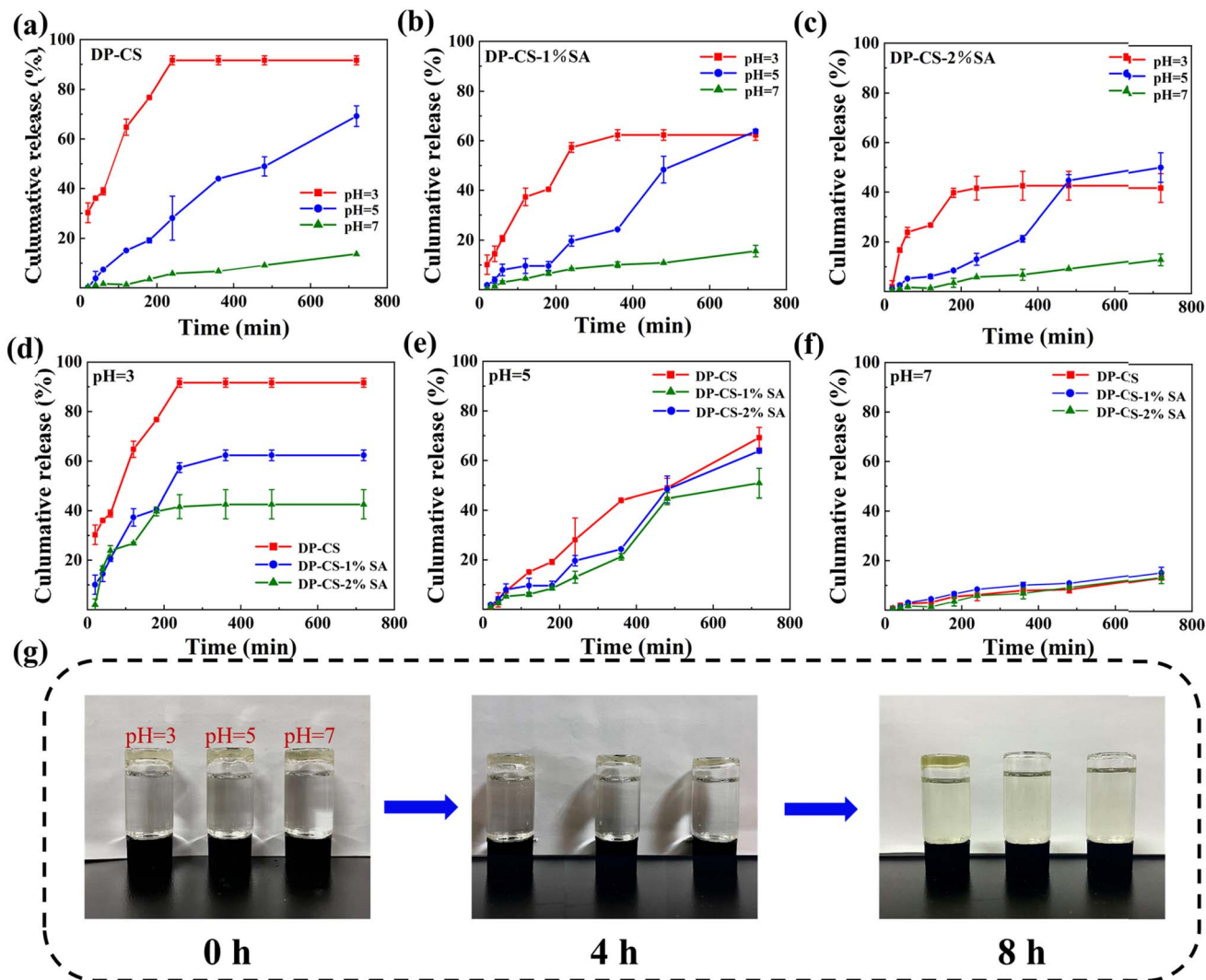
Fig. 6 (a)–(c) Baicalin-release rates from DP–CS, DP–CS–1%SA, and DP–CS–2%SA in PBS at different pH values; (d)–(f) Baicalin-release rates from DP–CS, DP–CS–1%SA, and DP–CS–2%SA in PBS at the same pH; (g) Baicalin-release experiment of DP–CS–2%SA in PBS at different pH values.

increase in time, the Schiff base bond decreased gradually, and the influence of electrostatic force on drug release increased.[11,12] The release rate of DP–CS–2%SA at pH = 5 gradually exceeded that at pH = 3, which indicates that the drug release can be regulated by introducing SA.

Fig. 6(g) shows images from the baicalin-release experiment using DP–CS–2%SA in PBS at different pH values. After 8 h, DP–CS–2%SA was almost completely dissolved at pH 3 and 5, whereas DP–CS–2%SA was barely dissolved at pH 7. This indicates that the DP–CS–2%SA hydrogel has good pH responsiveness and can achieve controlled drug release under different pH conditions.

3.7. Biocompatibility analysis

To further investigate the applicability of the drug-loaded DP–CS–2%SA hydrogel in biomedical applications, a CCK-8 assay was used to determine the cell viability. As shown in Fig. 7(a and b), cell viability was high in all groups after 1 and 3 days of

culture, indicating that the hydrogel is nontoxic to L929 cells. Fig. 7(c) shows the proliferation of L929 cells under an inverted microscope after 1 and 3 days of culture. The proliferation rate of cells cultured with the baicalin-loaded DP–CS–2%SA hydrogel for 3 days was significantly higher than that after 1 day, which is consistent with the results of the CCK-8 assay. Cells cultured with DP–CS–2% SA were mostly spindle-shaped or polygonal, indicating stronger cell activity. The cell density was higher under electron microscopy, suggesting that the prepared drug-loaded DP–CS–2%SA hydrogel is potentially a biocompatible drug carrier.

3.8. *In Vitro* antimicrobial activity analysis

To further investigate the medical applications of the baicalin-loaded DP–CS–2%SA hydrogel, its antibacterial properties were tested using a zone inhibition assay. As shown in Fig. 7(d), blank DP–CS–2%SA and baicalin-loaded DP–CS–2%SA hydrogel blocks were placed on a culture dish covered with *S. aureus* and
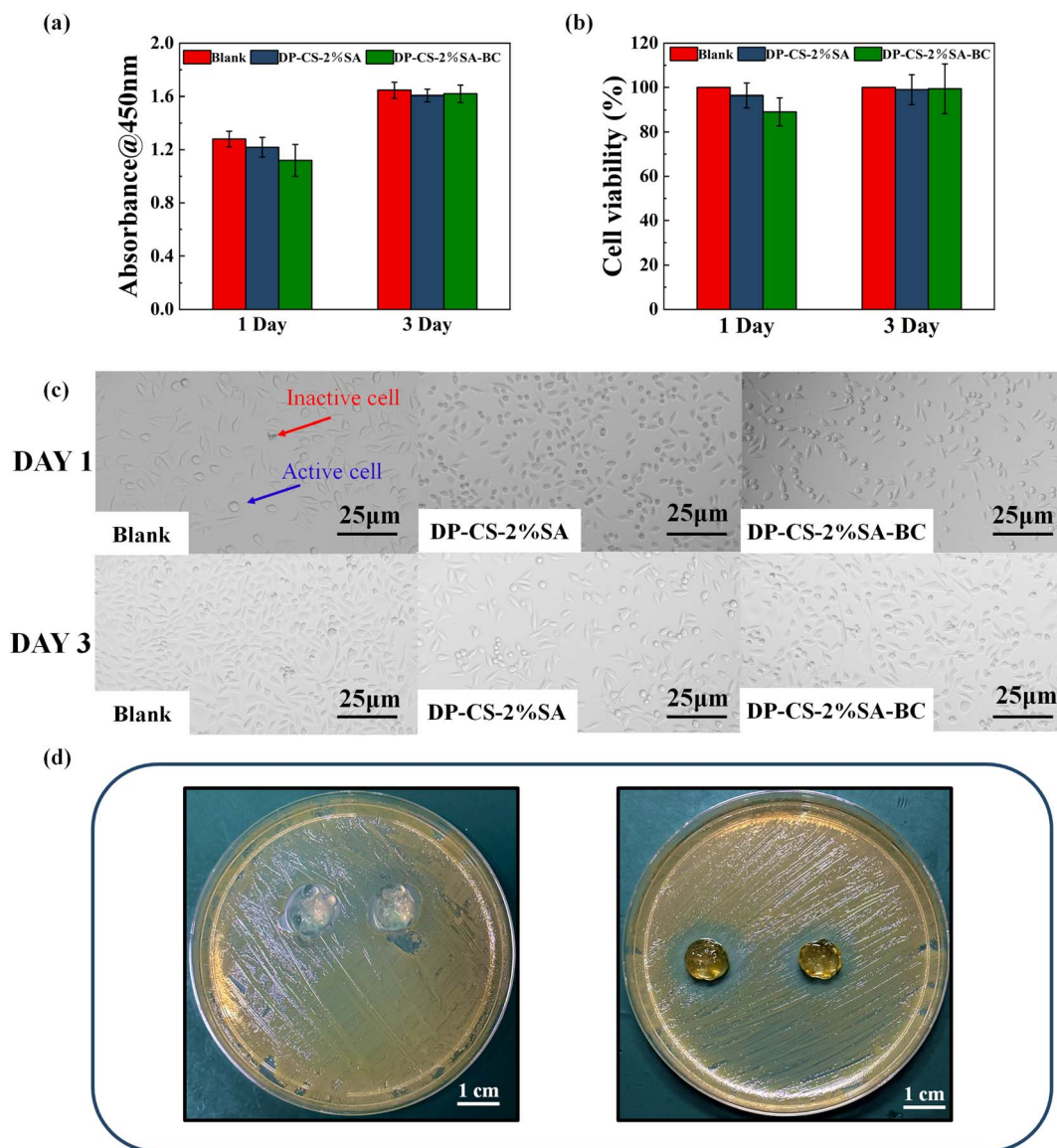
Fig. 7 Biocompatibility evaluation and *in vitro* antimicrobial activity of hydrogel materials: (a) measurement of the OD450 nm values of L929 cells at 1 and 3 days for the blank group and the DP−CS−2%SA and DP−CS−2%SA drug-loaded hydrogel groups; (b) cell viability of L929 cells after incubation for 1 and 3 days in the blank group and the DP−CS−2%SA and DP−CS−2%SA drug-loaded hydrogel groups; (c) morphology of cells in the blank group and the DP−CS−2%SA and DP−CS−2%SA drug-loaded hydrogel groups; (d) images of the inhibition ring on the blank DP−CS−2%SA and baicalin-loaded DP−CS−2%SA hydrogel.

incubated at 37 °C for 24 hours. The diameter of the inhibition zone for the baicalin-loaded DP−CS−2%SA hydrogel was 16–20 mm, which was significantly larger than that of the blank DP−CS−2%SA hydrogel. This indicates that baicalin can still exhibit antibacterial activity within the hydrogel, further demonstrating that the DP−CS−2%SA hydrogel is an effective drug carrier for biomedical applications.

4. Conclusion

In this study, we successfully constructed a pH-responsive dual-network biopolysaccharide hydrogel DP−CS−2%SA with enhanced self-healing and controlled drug release properties.

Through physical and chemical cross-linking, this material forms a network structure with excellent mechanical properties and self-healing characteristics. The rheological analysis confirmed that the double-network structure endows the hydrogel with high G' and G'', indicating its significant advantages in mechanical strength, stability and excellent self-healing ability. The swelling experiments further confirmed that the hydrogel exhibits excellent swelling properties, which are crucial for maintaining its functionality in the body. More importantly, *in vitro* drug-release experiments showed that as the SA content increased, the controlled release effect of the hydrogel became more pronounced, suggesting the possibility of designing drug delivery systems with specific release

characteristics. In addition, the biocompatibility and *in vitro* antimicrobial activity tests showed that the prepared hydrogel had no obvious toxicity to L929 cells and could exert the antimicrobial properties of baicalin, confirming its potential as a drug carrier material.

In conclusion, the dual-network self-healing biopolysaccharide hydrogel prepared in this study has excellent pH-regulated drug release ability. This system has practical application value in the precise controlled release of drugs.

Data availability

The data that support the findings of this study are available from the corresponding author upon reasonable request.

Author contributions

Conceptualization, Yuan Ma, Xiaoyong Qiu and Jun Huang; funding acquisition, Yunfeng Tang, Jianwei Fan, Tianyu Sun and Xiaolai Zhang; investigation, Yunfeng Tang, Jianwei Fan and Tianyu Sun; project administration, Yunfeng Tang, Jianwei Fan, Tianyu Sun and Xiaolai Zhang; resources, Xiaoyong Qiu and Jun Huang; validation, Yuan Ma and Luxing Wei; writing–original draft, Yuan Ma; writing–review & editing, Xiaoyong Qiu, Luxing Wei, Jun Huang and Xiaolai Zhang.

Conflicts of interest

There are no conflicts to declare.

Acknowledgements

References

1 X. Che, *et al.*, Application of Chitosan-Based Hydrogel in Promoting Wound Healing: A Review, *Polymers*, 2024, **16**(3), 344.

2 J. H. Yoon, *et al.*, Highly self-healable and flexible cable-type pH sensors for real-time monitoring of human fluids, *Biosens. Bioelectron.*, 2020, **150**, 111946.

3 H. Ozay, P. Ilgin and O. Ozay, Novel hydrogels based on crosslinked chitosan with formyl-phosphazene using Schiff-base reaction, *Int. J. Polym. Mater.*, 2021, **70**(4), 246–255.

4 Z. Wang, *et al.*, Dynamic covalent hydrogel of natural product baicalin with antibacterial activities†, *RSC Adv.*, 2022, **12**(14), 8737–8742; †Electronic supplementary information (ESI) available. See DOI: 10.1039/d1ra07553e. .

5 H. Du, *et al.*, The design of pH-sensitive chitosan-based formulations for gastrointestinal delivery, *Drug Discovery Today*, 2015, **20**(8), 1004–1011.

6 Y. J. Zhu and F. Chen, pH-Responsive Drug-Delivery Systems, *Chem.–Asian J.*, 2015, **10**(2), 284–305.

7 C. J. Roberts, *et al.*, Dissolution behavior of porcine somatotropin with simultaneous gel formation and lysine Schiff-base hydrolysis, *J. Control Release*, 2001, **77**(1–2), 107–116.

8 Q. Zhou, *et al.*, Baicalein and hydroxypropyl-γ-cyclodextrin complex in poloxamer thermal sensitive hydrogel for vaginal administration, *Int. J. Pharm.*, 2013, **454**(1), 125–134.

9 Y. Huang, *et al.*, Mechanical enhancement of graphene oxide-filled chitosan-based composite hydrogels by multiple mechanisms, *J. Mater. Sci.*, 2020, **55**(29), 14690–14701.

10 L. Chen, *et al.*, Preparation and properties of chitosan/dialdehyde sodium alginate/dopamine magnetic drug-delivery hydrogels, *Colloids Surf., A*, 2024, **680**, 132739.

11 H. Jing, *et al.*, Facile synthesis of pH-responsive sodium alginate/carboxymethyl chitosan hydrogel beads promoted by hydrogen bond, *Carbohydr. Polym.*, 2022, **278**, 118993.

12 H. Zhang, *et al.*, pH-sensitive O-carboxymethyl chitosan/sodium alginate nanohydrogel for enhanced oral delivery of insulin, *Int. J. Biol. Macromol.*, 2022, **223**, 433–445.

13 N. M. B. Ladeira, *et al.*, Preparation and characterization of hydrogels obtained from chitosan and carboxymethyl chitosan, *J. Polym. Res.*, 2021, **28**(9), 335.

14 A. M. Craciun, S. Morariu and L. Marin, Self-Healing Chitosan Hydrogels: Preparation and Rheological Characterization, *Polymers*, 2022, **14**(13), 2570.

15 K. Kiti and O. Suwantong, Bilayer wound dressing based on sodium alginate incorporated with curcumin-β-cyclodextrin inclusion complex/chitosan hydrogel, *Int. J. Biol. Macromol.*, 2020, **164**, 4113–4124.

16 Z. Feyisa, *et al.*, Fabrication of pH-sensitive double cross-linked sodium alginate/chitosan hydrogels for controlled release of amoxicillin, *Polym. Eng. Sci.*, 2023, **63**(8), 2546–2564.

17 A. Wang, *et al.*, Transcriptome Sequencing Explores the Mechanism of Baicalin on Bone Cancer Pain, *J. Inflammation Res.*, 2021, **14**, 5999–6010.

18 L. Wei, *et al.*, An underwater stable and durable gelatin composite hydrogel coating for biomedical applications, *J. Mater. Chem. B*, 2023, **11**(47), 11372–11383.

19 Y. Chen, *et al.*, Preparation and characterization of a novel antibacterial hydrogel based on thiolated ovalbumin/gelatin with silver ions, *Innovative Food Sci. Emerging Technol.*, 2022, **78**, 103007.

20 B. Yan, *et al.*, Duplicating Dynamic Strain-Stiffening Behavior and Nanomechanics of Biological Tissues in a Synthetic Self-Healing Flexible Network Hydrogel, *ACS Nano*, 2017, **11**(11), 11074–11081.

21 X. Yang, *et al.*, Highly Efficient Self-Healable and Dual Responsive Cellulose-Based Hydrogels for Controlled Release and 3D Cell Culture, *Adv. Funct. Mater.*, 2017, **27**(40), 1703174.

22 Q. Zhang, *et al.*, A uniform-unsaturated crosslinking strategy to construct injectable alginate hydrogel, *Int. J. Biol. Macromol.*, 2024, **254**, 127726.

23 B. L. Guo, J. F. Yuan and Q. Y. Gao, Preparation and release behavior of temperature-and pH-responsive chitosan material, *Polym. Int.*, 2008, **57**(3), 463–468.

24 M. Fan, *et al.*, Biodegradable hyaluronic acid hydrogels to control release of dexamethasone through aqueous Diels-Alder chemistry for adipose tissue engineering, *Mater. Sci. Eng. C*, 2015, **56**, 311–317.

25 X. Qiu, *et al.*, Multi-functional rhodamine-based chitosan hydrogels as colorimetric Hg2+ adsorbents and pH-triggered biosensors, *J. Colloid Interface Sci.*, 2021, **604**, 469–479.

26 S. R. Derkach, *et al.*, Interactions between gelatin and sodium alginate: UV and FTIR studies, *J. Dispersion Sci. Technol.*, 2020, **41**(5), 690–698.

27 J. Wang, *et al.*, Synthesis and antimicrobial activity of Schiff base of chitosan and acylated chitosan, *J. Appl. Polym. Sci.*, 2012, **123**(6), 3242–3247.

28 S. Honary, M. Maleki and M. Karami, The effect of chitosan molecular weight on the properties of alginate/chitosan microparticles containing prednisolone, *Trop. J. Pharm. Res.*, 2009, **8**(1), 53–61.

29 A. K. Jangid, *et al.*, Solid-state properties, solubility, stability and dissolution behaviour of co-amorphous solid dispersions of baicalin, *CrystEngComm*, 2020, **22**(37), 6128–6136.

30 G. Liu, Z. Bao and J. Wu, Injectable baicalin/F127 hydrogel with antioxidant activity for enhanced wound healing, *Chin. Chem. Lett.*, 2020, **31**(7), 1817–1821.

31 G. Yu, *et al.*, Preparation and Properties of Self-Cross-Linking Hydrogels Based on Chitosan Derivatives and Oxidized Sodium Alginate, *ACS Omega*, 2023, **8**(22), 19752–19766.

32 Z. Su, *et al.*, Mussel-Inspired Calcium Alginate/Polyacrylamide Dual Network Hydrogel: A Physical Barrier to Prevent Postoperative Re-Adhesion, *Polymers*, 2023, **15**(23), 4498.

33 X. Chen, *et al.*, Magnetic and self-healing chitosan-alginate hydrogel encapsulated gelatin microspheres via covalent cross-linking for drug delivery, *Mater. Sci. Eng., C*, 2019, **101**, 619–629.

34 S. Pan, *et al.*, Chitosan-Based Self-Healing Hydrogel: From Fabrication to Biomedical Application, *Polymers*, 2023, **15**(18), 3768.

35 P. Bertsch, *et al.*, Self-Healing Injectable Hydrogels for Tissue Regeneration, *Chem. Rev.*, 2023, **123**(2), 834–873.

36 T. Funami, *et al.*, Rheological properties of sodium alginate in an aqueous system during gelation in relation to supermolecular structures and Ca2+ binding, *Food Hydrocolloids*, 2009, **23**(7), 1746–1755.

37 S. Fu, *et al.*, Relevance of rheological properties of sodium alginate in solution to calcium alginate gel properties, *AAPS PharmSciTech*, 2011, **12**(2), 453–460.